**GSA Data Repository 2015042**

**Supplementary Files - Figure SF1A:** Complete stratigraphic column for core LT24 (after Orpin et al., 2010). Earthquake-triggered homogenites are shown by purple and storm-triggered homogenites by red shading. N.B. Only the most pronounced textural changes that separate and subdivide the >3000 individual units are shown at this scale. More detail is visible in the expanded section (250 – 300 cm) shown in Figure SF1B.

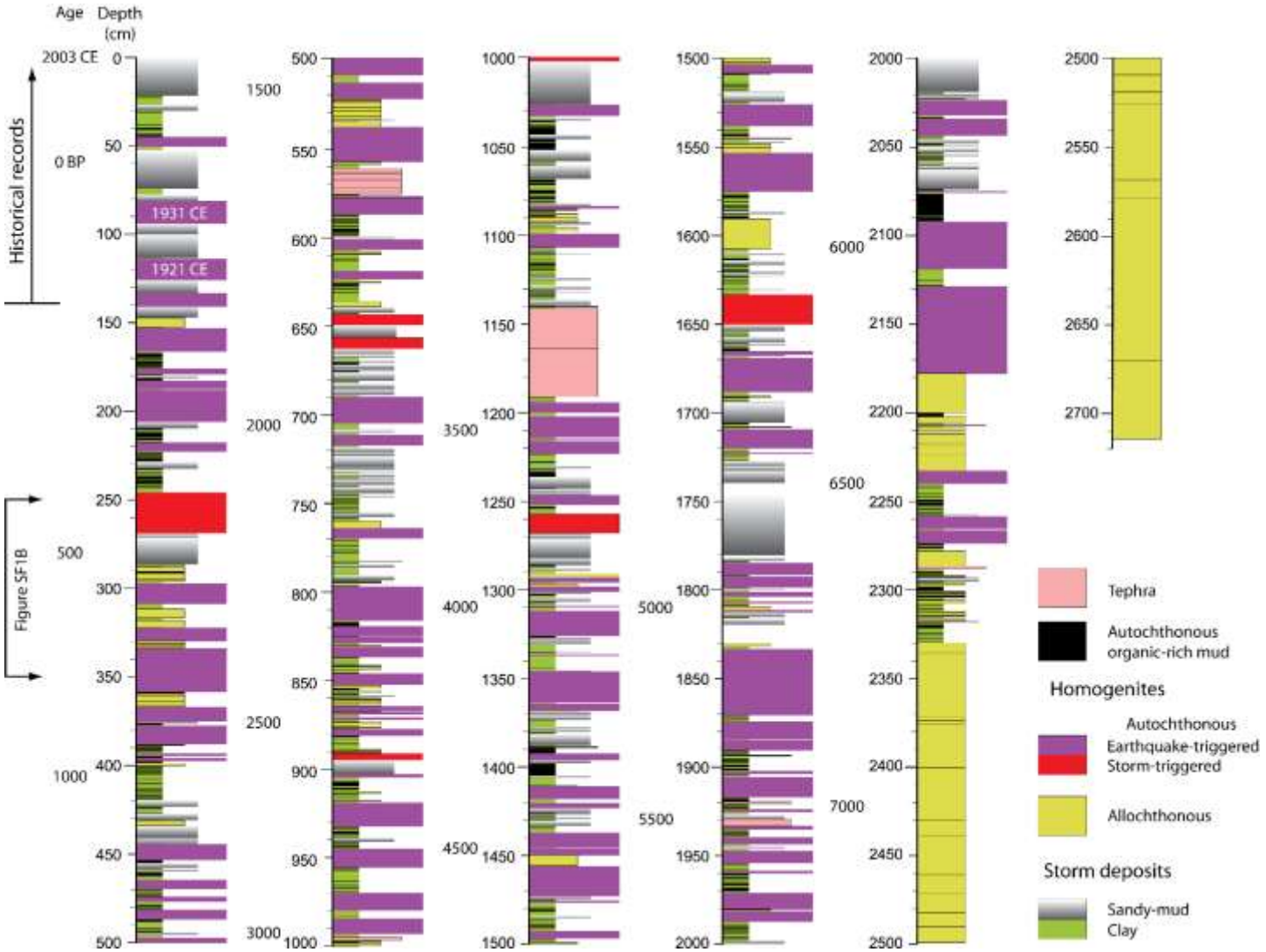

**Figure SF1B:** Expanded section of the stratigraphic column (Figure SF1A) and corresponding core photographs showing the juxtaposition of a graded storm deposit and a storm-triggered homogenite unit (shown in red). Graded storm deposits are the result of high magnitude rainfalls above the threshold for shallow landslides, which then dominate the sediment supply. Shallow landslides erode regolith ≤ 1 m deep, that comprises a range of particle sizes. The graded storm deposits are the result of the differential settling of these particle sizes within the lake (Page et al., 2010), and this homogenite is presumed to have been created because the terrigenous inputs overloaded the lake-margin. Such situations occur relatively infrequently in the prehistoric sediment record, and the autochthonous homogenite stratigraphy (see Figure SF1A) is dominated by earthquake-triggered events (shown in purple). In the last century, historical records of storm and earthquake activity in the Hawke's Bay region permit us to differentiate between storm- and earthquake-triggered homogenites.

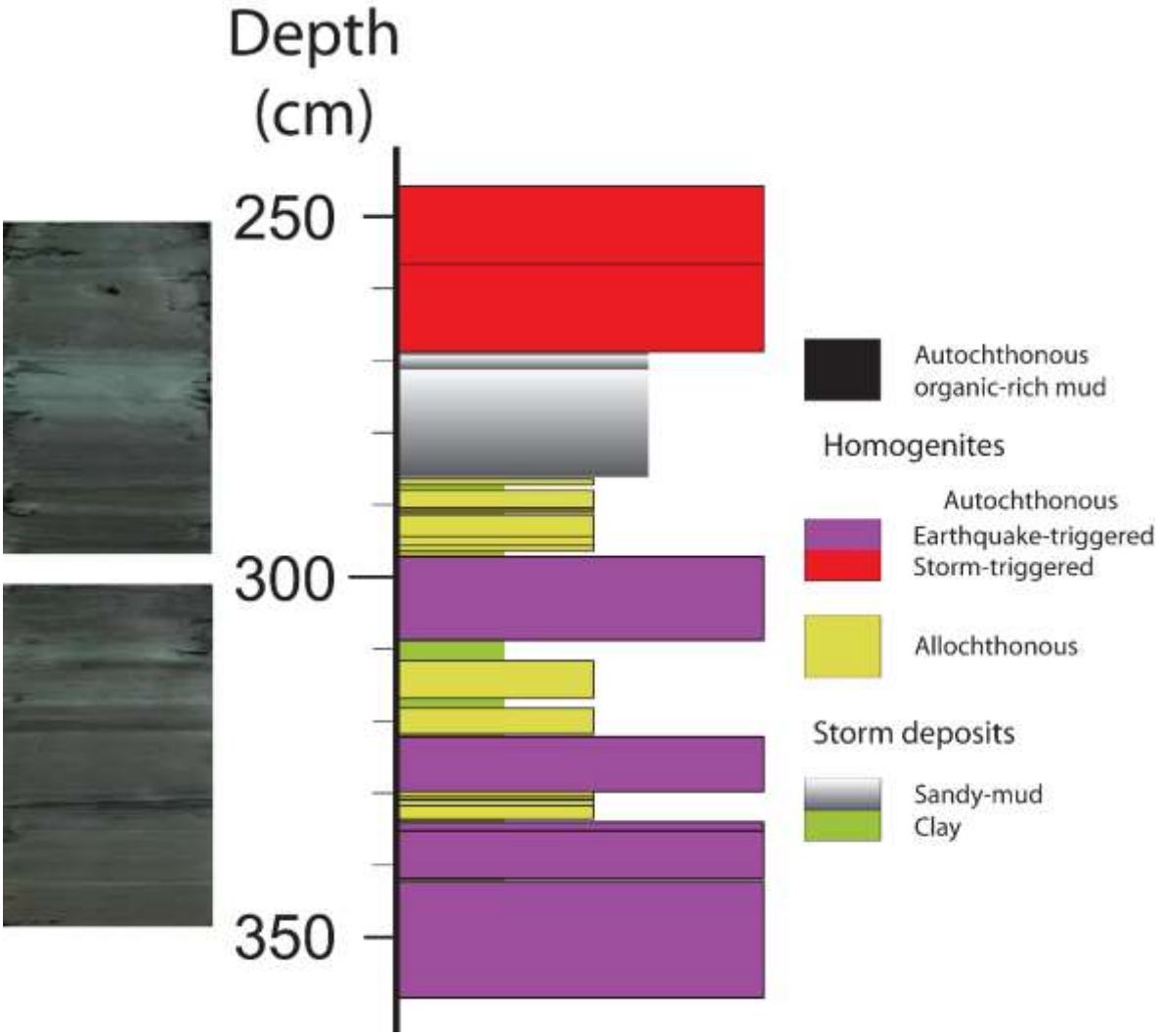

**Table SF1:** Age and time between earthquake-triggered homogenites in Lake Tutira sediment core LT24. Underlining indicates homogenites that are believed to be associated with paleoearthquakes on the subduction interface and Lachlan Fault (see Table SF2), and bold type homogenites that correlate with the historical 1931 and 1921 Hawke's Bay earthquakes. Earthquake-triggered homogenites and storm deposits respectively account for ~30% and ~26% of the total thickness (27.14 m) of sediment recovered in core LT24, and the core stratigraphy is described in Orpin et al. (2010) and Page et al. (2010) and summarized in Figure SF1A. Uncertainties (± 2σ) associated with the linear model used estimate the calendar ages of depths in core LT24 are also portrayed in Figure SF2.

| **Homogenite age (Cal. yr BP ±2σ)** | **Waiting time (Yr)** | **Homogenite age (Cal. yr BP ±2σ)** | **Waiting time (Yr)** | **Homogenite age (Cal. yr BP ±2σ)** | **Waiting time (Yr)** | **Homogenite age (Cal. yr BP ±2σ)** | **Waiting time (Yr)** |
|---|---|---|---|---|---|---|---|
| 3 ±2 | 17 | 1720 ±13 | 0 | 3438 ±30 | 71 | 4807 ±158 | 37 |
| **20 ±2** | 10 | 1720 ±13 | 2 | 3509 ±33 | 7 | 4844 ±163 | 5 |
| **30 ±2** | 28 | 1722 ±13 | 15 | 3516 ±34 | 42 | 4849 ±159 | 111 |
| 58 ±4 | 89 | 1737 ±14 | 34 | 3558 ±38 | 146 | 4960 ±108 | 12 |
| 147 ±13 | 44 | 1771 ±17 | 29 | 3704 ±57 | 210 | 4972 ±104 | 8 |
| 191 ±17 | 29 | 1800 ±22 | 140 | 3913 ±88 | 15 | 4980 ±101 | 6 |
| 219 ±21 | 19 | 1940 ±53 | 22 | 3929 ±91 | 26 | 4987 ±100 | 8 |
| 238 ±23 | 15 | 1961 ±57 | 91 | 3954 ±94 | 45 | 4995 ±98 | 95 |
| 253 ±24 | 30 | 2052 ±78 | 81 | 4000 ±102 | 83 | 5090 ±94 | 22 |
| 283 ±28 | 59 | 2133 ±78 | 61 | 4083 ±113 | 58 | 5111 ±99 | 11 |
| 342 ±34 | 298 | 2194 ±73 | 4 | 4141 ±125 | 94 | 5122 ±103 | 104 |
| 640 ±67 | 85 | 2198 ±74 | 31 | 4235 ±143 | 48 | 5226 ±78 | 131 |
| 725 ± 67 | 22 | 2229 ±72 | 16 | 4283 ±148 | 2 | 5357 ±52 | 77 |
| 747 ±65 | 28 | 2245 ±72 | 29 | 4285 ±148 | 9 | 5434 ±43 | 4 |
| 775 ±64 | 69 | 2274 ±72 | 37 | 4294 ±150 | 3 | 5438 ±43 | 87 |
| 844 ±59 | 69 | 2310 ±72 | 21 | 4296 ±150 | 3 | 5525 ±46 | 23 |
| 914 ±55 | 48 | 2332 ±72 | 54 | 4299 ±150 | 118 | 5548 ±46 | 29 |
| 962 ±52 | 7 | 2386 ±74 | 9 | 4418 ±151 | 30 | 5577 ±49 | 16 |
| 969 ±51 | 27 | 2394 ±75 | 11 | 4448 ±146 | 9 | 5593 ±51 | 57 |
| 996 ±50 | 12 | 2405 ±76 | 33 | 4456 ±142 | 9 | 5650 ±66 | 18 |
| 1008 ±49 | 234 | 2438 ±79 | 87 | 4466 ±137 | 38 | 5668 ±73 | 125 |
| 1242 ±33 | 50 | 2525 ±89 | 94 | 4504 ±123 | 8 | 5793 ±117 | 32 |
| 1292 ±31 | 3 | 2619 ±101 | 7 | 4513 ±123 | 41 | 5825 ±128 | 89 |
| 1295 ±30 | 16 | 2627 ±102 | 87 | 4553 ±113 | 7 | 5913 ±162 | 118 |
| 1311 ±30 | 29 | 2713 ±116 | 87 | 4560 ±113 | 36 | 6032 ±209 | 163 |
| 1340 ±28 | 42 | 2800 ±131 | 51 | 4596 ±116 | 19 | 6195 ±277 | 308 |
| 1382 ±25 | 86 | 2851 ±139 | 62 | 4615 ±120 | 53 | 6503 ±197 | 176 |
| 1468 ±21 | 56 | 2913 ±119 | 231 | 4667 ±136 | 39 | 6679 ±141 | 57 |
| 1525 ±16 | 113 | 3144 ±78 | 69 | 4706 ±126 | 82 | 6736 ±140 | – |
| 1638 ±15 | 82 | 3213 ±63 | 225 | 4788 ±144 | 19 | | |

**Table SF2:** Chronology of major to great paleoearthquakes in the Hawke's Bay region derived from on terrestrial records of records of coastal uplift and subsidence (after Berryman, 1993; Cochran et al., 2006; Hayward et al., 2006), and corresponding uncertainties in the age estimates (N.J. Litchfield, personal commun.).

| Calibrated Age (Cal. yr BP) | Uncertainty (± Cal. yr BP) | Earthquake source |
|---|---|---|
| 250 | 100 | Lachlan Fault |
| 600 | 300 | Subduction interface |
| 1400 | 100 | Lachlan Fault |
| 1600 | 100 | Subduction interface |
| 1820 | 40 | Lachlan Fault |
| 2950 | 100 | Subduction interface |
| 3400 | 100 | Lachlan Fault |
| 4200 | 300 | Subduction interface |
| 5550 | 60 | Lachlan Fault |
| 5800 | 100 | Subduction interface |

**Figure SF2:** Uncertainties (95% confidence intervals shown by grey envelopes) in Orpin et al's (2010) linear age-depth model for core LT24, calculated using a Monte Carlo approach (10,000 iterations; Blaauw, 2010), from the calibrated age distribution of 12 tephras (green histograms), the calibrated $^{14}C$ age of wood fragments from near the base of the core (blue histogram), and the known dates of four storms in the historic record (red bars). Arrows indicate tephras on which Pouderoux et al's (2012) turbidite chronology for core MD06-3003 also relies (see Table SF3).

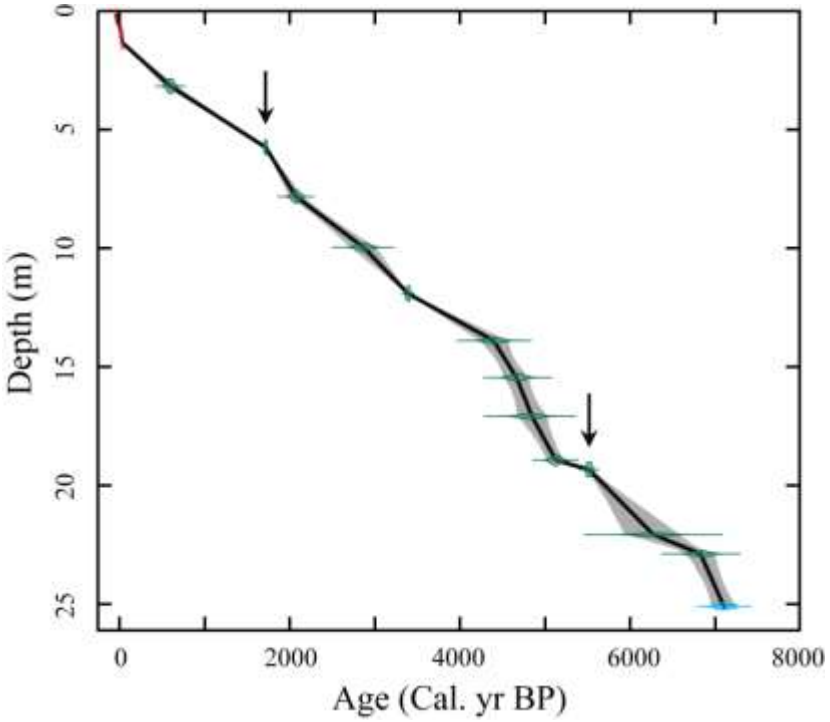

**Table SF3:** Age at the base of turbidites in core MD06-3003. Pouderoux et al's (2012) turbidite chronology was determined from the hemipelagite sedimentation rate, by linear interpolation between the calendar ages for tephras erupted from the Taupo Volcanic Zone, which also function as tie points for intercorrelation with core LT24 (see Figure SF2), and calibrated $^{14}C$ ages from mixed planktonic foraminifers.

| **Turbidite age (Cal. Yr BP ±2σ)** |
|---|
| 915 ±168 |
| 1358 ±140 |
| 1717 ±13 |
| 2214 ±113 |
| 2260 ±122 |
| 2441 ±158 |
| 2753 ±182 |
| 2931 ±189 |
| 3234 ±178 |
| 3428 ±168 |
| 4333 ±121 |
| 4657 ±105 |
| 4786 ±98 |
| 4851 ±95 |
| 5045 ±85 |
| 5498 ±62 |
| 5558 ±60 |
| 5614 ±59 |
| 5643 ±59 |
| 5755 ±59 |
| 5980 ±57 |
| 6036 ±57 |
| 6599 ±54 |
| 6711 ±53 |
| 6824 ±52 |

**References**


Berryman, K.R., 1993. Age, height, and deformation of Holocene marine terraces at Mahia Peninsula, Hikurangi Subduction Margin, New Zealand, Tectonics, v. 12, 1347–1364.

Blaauw, M., 2010, Methods and code for 'classical' age-modelling of radiocarbon sequences, Quaternary Geochronology, v. 5, 512–518.

Cochran, U., Berryman, K., Mildenhall, D.C., Hayward, B.W., Southall, K., Hollis, C.J., Barker, P., Wallace, L., Alloway, B.V. and Wilson, K., 2006, Paleoecological insights into subduction zone earthquake occurrence, eastern North Island, New Zealand, Geological Society of America Bulletin, v. 118, 1051–1074.

Hayward, B. W., Grenfell, H.R., Sabaa, A.T., Carter, R., Cochran, U., Lipps, J.H., Shane, P.R. and Morley, M.S., 2006, Micropaleontological evidence of large earthquakes in the past 7200 years in southern Hawke's Bay, New Zealand, Quaternary Science reviews, v. 25, 1186–1207.

Orpin, A. Carter, L., Page, M.J., Cochran, U.A., Trustrum, N.A., Gomez, B., Palmer, A.S., Mildenhall, D.C., Rogers, K.M., Brackley, H.L., and Northcote, L., 2010, Holocene sedimentary record from Lake Tutira: A template for upland watershed erosion proximal to the Waipaoa Sedimentary System, north-eastern New Zealand, Marine Geology, v. 270, 11–29, doi:10.1016/j.margeo.2009.10.022.

Page, M.J. Trustrum, N.A., Orpin, A.R., Carter, L., Gomez, B., Cochran, U.A., Mildenhall, D.C., Rogers, K.M., Brackley, H.L., Palmer, A.S., and Northcote, L., 2010, Storm frequency and magnitude in response to Holocene climate variability, Lake Tutira, north-eastern New Zealand, Marine Geology, v. 270, 30–44, doi:10.1016/j.margeo.2009.10.019.

Pouderoux, H., Proust, J-N., Lamarche, G., Orpin, A., and Neil, H., 2012, Postglacial (after 18 ka) deep-sea sedimentation along the Hikurangi subduction margin (New Zealand): Characterisation, timing and origin of turbidites, Marine Geology, v. 295–298, 51–76, doi:10.1016/j.margeo.2011.11.002.